Advanced Structured Materials

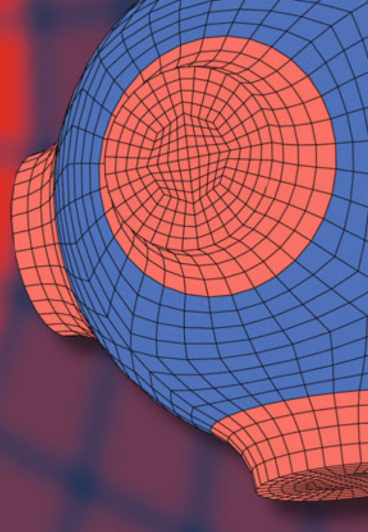

Wolfgang H. Müller
Alfons Noe
Ferdinand Ferber *Editors*

New Achievements in Mechanics

A Tribute to Klaus Peter Herrmann

Springer

Advanced Structured Materials

Volume 205

Wolfgang H. Müller · Alfons Noe ·
Ferdinand Ferber
Editors

New Achievements in Mechanics

A Tribute to Klaus Peter Herrmann

Springer

Editors
Wolfgang H. Müller
Institute of Mechanics
Technical University of Berlin
Berlin, Germany

Ferdinand Ferber
Faculty of Mechanical Engineering
Paderborn University
Paderborn, Germany

Alfons Noe
Department of Mechanical Engineering
South Westphalia University of Applied Sciences
Soest, Germany

ISSN 1869-8433 ISSN 1869-8441 (electronic)
Advanced Structured Materials
ISBN 978-3-031-56131-3 ISBN 978-3-031-56132-0 (eBook)
https://doi.org/10.1007/978-3-031-56132-0

This Springer imprint is published by the registered company Springer Nature Switzerland AG
The registered company address is: Gewerbestrasse 11, 6330 Cham, Switzerland

Paper in this product is recyclable.

Contents

Electrically Permeable Interface Crack with a Contact Zone in a 1D Piezoelectric Quasicrystal

Volodymyr V. Loboda, Volodymyr B. Govorukha, and Alla E. Sheveleva

Abstract The bimaterial composed of two 1D piezoelectric hexagonal quasicrystals having a crack along the material interface is considered. Mixed mode phonon and phason remote loading resulting from the plane strain conditions at infinity are applied. The phonon field represents the lattice vibrations similar to crystals while the phason field depicts the quasi-periodic rearrangement of atoms inherent for quasicrystals. Because in the framework of the open crack model the electromechanical fields have an oscillating singularity at the crack tips, therefore, the artificial contact zone model is considered. Introducing the artificial contact zone at the right crack tip the problem is reduced to a combination of combined Dirichlet—Riemann and Hilbert boundary value problems. These problems are solved analytically for any length of the artificial contact zone. Clear analytical expressions for phonon and phason mechanical parameters are derived. The real contact zone is obtained from the satisfaction of the additional conditions that lead to the transcendental equations with respect to the relative contact zone length. After solving these equations, the stress intensity factors and the energy release rates are found analytically.

V. V. Loboda (✉)
Department of Theoretical and Computational Mechanics, Oles Honchar Dnipro National University, Gagarin Av., 72, Dnipro 49010, Ukraine
e-mail: loboda@dnu.dp.ua

V. B. Govorukha
Department of Higher Mathematics, Physics and General Engineering Disciplines, Dnipro State Agrarian and Economic University, Serhii Efremov Str. 25, Dnipro 49600, Ukraine

A. E. Sheveleva
Department of Computational Mathematics and Mathematical Cybernetics, Oles Honchar Dnipro National University, Gagarin Av., 72, Dnipro 49010, Ukraine
e-mail: shevelevaae@dnu.dp.ua

W. H. Müller et al. (eds.), *New Achievements in Mechanics*, Advanced Structured Materials 205, https://doi.org/10.1007/978-3-031-56132-0_7

1 Introduction

The quasicrystaline materials, found by Shechtman et al. [1] are nowadays extensively used in various areas of technology and engineering. Particularly, quasicrystaline bi-materials with piezoelectric effect are applied in smart structures. In the most comprehensive form the generalized elasticity theory of quasicrystals (QCs) is given in [2]. Depending on the directions number of the atom arrangement quasiperiodicity, QCs can be categorized into three sub-classes, i.e. 1D, 2D and 3D [3]. One-dimensional (1D) quasicrystals exhibit one quasi-periodic axis, while the perpendicular plane reveals classical crystalline properties.

Crack analysis has been extended to mechanics of QCs in the recent decade and up to now, a lot of research efforts to crack analyses for QCs have been made. For example, using the mathematical theory of elasticity of QCs, Fan et al. [4] and Li et al. [5] studied the moving screw dislocation and straight dislocation in one-dimensional hexagonal QCs. Gao et al. [6] considered the problem of cubic quasicrystal media with an elliptic hole or a crack. Liu et al. [7] studied the interaction of dislocations with cracks in one-dimensional hexagonal QCs based on the analytic function theory. One-dimensional hexagonal quasicrystal with a planar crack in an infinite medium was studied in [8]. The method of crack path prediction under mixed-mode loading in 1D quasicrystals was developed in [9].

Piezoelectricity is an important physical property of QCs. Green's functions of one-dimensional quasicrystal bi-material with piezoelectric effect were investigated in [10]. A set of 3D general solutions to static problems of 1D hexagonal piezoelectric quasicrystals is obtained in [11] with use of displacement functions. Three-dimensional cracks in one-dimensional hexagonal piezoelectric quasicrystals were studied in [12] and a penny-shaped dielectric crack in the quasicrystal plate of the same structure was considered in [13]. Two asymmetrical limited permeable cracks emanating from an elliptical hole in one-dimensional hexagonal piezoelectric quasicrystals were considered in [14].

It is worth to be mentioned that interface cracks in bi-material and multi-material components are the main reason of failure. An open crack model for an interface crack in an isotropic bimaterial was investigated in [15] and the contact zone model for such crack was developed in [16]. Interface cracks with contact zones were considered for anisotropic [17], piezoelectric [18, 19] and piezoelectric/piezomagnetic [20] bimaterials by Professor Herrmann and his co-authors. Thermal fields for such problems were taken into account in [21–23]. Moving cracks between anisotropic and piezoelectric materials were considered in [24] and [25, 26], respectively. The influence of the electric permeability on an interface crack in a piezoelectric bimaterial was studied in [27, 28]. Interface cracks in piezoelectric bimaterials under compressed-shear loading were considered in [29, 30]. A polling direction influence on fracture parameters of a limited permeable interface crack in a piezoelectric bi-material was investigated in paper [31].

The cracks between different quasicrystals materials have not been sufficiently studied till now. To our knowledge an arbitrarily shaped electrically impermeable interface crack in an one-dimensional hexagonal thermo-electro-elastic quasicrystal bi-material was investigated in [32, 33] by an analytically-numerical method and a plane problem for an electrically permeable interface crack in a 1D piezoelectric QC was studied analytically in paper [34]. Multiple numbers of electrically permeable cracks on the interface between two one-dimensional piezoelectric quasicrystals were investigated in [35]. Besides, several publications related to the antiplane case of an interface crack in QCs were recently published. A crack between dissimilar one-dimensional hexagonal piezoelectric quasicrystals with electrically permeable and impermeable conditions at the crack faces under anti-plane shear and in-plane electric loadings was examined in [36]. An interface crack with mixed conducting-permeable electric conditions in a 1D piezoelectric quasi-crystalline space under the action of out of plane phonon and phason shear stresses and in-plane electric field was analytically considered in [37]. The problem of multiple collinear electrically permeable interface cracks between dissimilar one-dimensional hexagonal quasicrystals with piezoelectric effects under anti-plane shear and in-plane electric loading has been studied in [38].

It was shown in paper [34] that oscillating singularity appears at the crack tips of an electrically permeable interface crack considered in the framework of the open crack model in a 1D piezoelectric QC. It means that the contact zones take place at the crack tips in reality. To the authors knowledge contact zones for interface cracks in piezoelectric QCs have never been considered earlier. Studying of this problem is the main purpose of the present paper.

2 Formulation of the Problem and Constitutive Relations

Consider the plane problem in $(x_1, 0, x_3)$ plane for a crack $c \le x_1 \le b$, $x_3 = 0$ in the interface between two semi-infinite 1D piezoelectric hexagonal quasicrystalline spaces with $(x_1, 0, x_2)$ coincident with the periodic plane and the x_3-axis identical to the quasi-periodic direction (Fig. 1). In this figure c_{ij} and K_i are the elastic constants in the phonon and phason fields, respectively; the R_i represent the phonon–phason coupling elastic constants; e_{jk} and $\tilde{e}_{jk}$ are the piezoelectric constants in the phonon and phason fields, respectively; ξ_{ii} are the permittivity constants. It is assumed that the crack is electrically permeable and uniformly distributed phonon $(\sigma^{\infty}, \tau^{\infty})$ and phason H^{∞} stresses are prescribed at infinity.

The constitutive relations in this case have the form

$$\begin{Bmatrix} \sigma_{11} \\ \sigma_{33} \\ \sigma_{13} \end{Bmatrix} = \begin{bmatrix} c_{11} & c_{13} & 0 \\ c_{13} & c_{33} & 0 \\ 0 & 0 & 2c_{44} \end{bmatrix} \begin{Bmatrix} \varepsilon_{11} \\ \varepsilon_{33} \\ \varepsilon_{13} \end{Bmatrix} - \begin{bmatrix} 0 & e_{31} \\ 0 & e_{33} \\ e_{15} & 0 \end{bmatrix} \begin{Bmatrix} E_1 \\ E_3 \end{Bmatrix} + \begin{bmatrix} 0 & R_1 \\ 0 & R_2 \\ R_3 & 0 \end{bmatrix} \begin{Bmatrix} W_{31} \\ W_{33} \end{Bmatrix}, \tag{1}$$

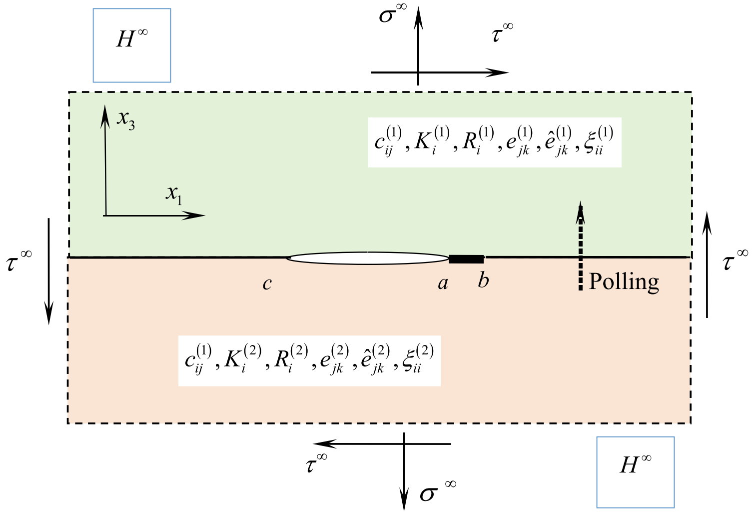

Fig. 1 A crack between two 1D piezoelectric QCs

$$\begin{Bmatrix} D_1 \\ D_3 \end{Bmatrix} = \begin{bmatrix} 0 & 0 & 2e_{15} \\ e_{31} & e_{33} & 0 \end{bmatrix} \begin{Bmatrix} \varepsilon_{11} \\ \varepsilon_{33} \\ \varepsilon_{13} \end{Bmatrix} + \begin{bmatrix} \xi_{11} & 0 \\ 0 & \xi_{33} \end{bmatrix} \begin{Bmatrix} E_1 \\ E_3 \end{Bmatrix} + \begin{bmatrix} \tilde{e}_{15} & 0 \\ 0 & \tilde{e}_{33} \end{bmatrix} \begin{Bmatrix} W_{31} \\ W_{33} \end{Bmatrix}, \quad (2)$$

$$\begin{Bmatrix} H_{31} \\ H_{33} \end{Bmatrix} = \begin{bmatrix} 0 & 0 & 2R_3 \\ R_1 & R_2 & 0 \end{bmatrix} \begin{Bmatrix} \varepsilon_{11} \\ \varepsilon_{33} \\ \varepsilon_{13} \end{Bmatrix} + \begin{bmatrix} K_2 & 0 \\ 0 & K_1 \end{bmatrix} \begin{Bmatrix} W_{31} \\ W_{33} \end{Bmatrix} - \begin{bmatrix} \tilde{e}_{15} & 0 \\ 0 & \tilde{e}_{33} \end{bmatrix} \begin{Bmatrix} E_1 \\ E_3 \end{Bmatrix}. \quad (3)$$

The equilibrium equations and geometric equations are the following

$$\sigma_{11,1} + \sigma_{13,3} = 0, \sigma_{31,1} + \sigma_{33,3} = 0, D_{1,1} + D_{3,3} = 0, H_{31,1} + H_{33,3} = 0, \quad (4)$$

$$\varepsilon_{ij} = \frac{1}{2}(u_{i,j} + u_{j,i}), E_i = -\varphi_{,i}, W_{3i} = W_{3,i}. \quad (5)$$

Herein $i, j = 1, 3$ and the denotation "," represents the derivative operation for the space variables; u_i, W_3 and φ are the phonon displacements, the phason displacement, and the electric potential, respectively; the atom arrangement is periodic in the $x_1 - x_2$ plane and quasi-periodic in the x_3-axis; σ_{ij} and ε_{ij} are the phonon stresses and strains, respectively; H_{3i} and W_{3i} are the phason stresses and strains, respectively; D_i and E_i are the electric displacements and electric fields, respectively; the polarization direction is along the x_3-axis.

It is also assumed that the crack surfaces are traction-free for $x_1 \in [c, a] = L_1$ whereas they are in frictionless contact for $x_1 \in (a, b) = L_2$, and the position of the point a is arbitrarily chosen for the time being. Such assumption means that we'll consider only one zone of the crack faces contact. In reality such zones arise at both interface crack tips [15], but one of them is usually extremely short and its influence upon the longer contact zone is negligibly small [18]. It should be emphasized as well that the longer contact zone arises at the right crack (point b in our case) tip for $\tau^{\infty} > 0$ if the lower material is "softer" then the upper one and it arises there for $\tau^{\infty} < 0$ in the opposite case. Without loss of generality the last alternative is used in this paper for definiteness.

The interface conditions can be written in the following form

$$\sigma_{13}^{\pm} = 0, \quad \sigma_{33}^{\pm} = 0, \quad H_{33}^{\pm} = 0, \quad \langle \varphi \rangle = 0, \quad \langle D_3 \rangle = 0 \text{ for } c < x_1 < a \tag{6}$$

$$\begin{gathered} \sigma_{13} = 0, \langle u_3 \rangle = 0, \ \langle W_3 \rangle = 0, \langle \sigma_{33} \rangle = 0, \\ \langle H_{33} \rangle = 0, \ \langle \varphi \rangle = 0, \ \langle D_3 \rangle = 0 \text{ for } x_1 \in (a, b) \end{gathered} \tag{7}$$

$$\begin{gathered} \langle \sigma_{13} \rangle = 0, \langle \sigma_{33} \rangle = 0, \langle H_{33} \rangle = 0, \langle u_1 \rangle = 0, \langle u_3 \rangle = 0, \\ \langle W_3 \rangle = 0, \langle \varphi \rangle = 0, \ \langle D_3 \rangle = 0 \text{ for } x_1 \notin (c, b). \end{gathered} \tag{8}$$

In paper [34] the following expressions were obtained

$$\sigma_{33}^{(1)}(x_1, 0) + m_{j5} H_{33}^{(1)}(x_1, 0) + i \cdot m_{j1} \sigma_{13}^{(1)}(x_1, 0) = \Theta_j^+(x_1) + \gamma_j \Theta_j^-(x_1), \tag{9}$$

$$n_{j1} \langle u_1'(x_1) \rangle + i \cdot n_{j3} \langle u_3'(x_1) \rangle + i \cdot n_{j5} \langle W_3'(x_1) \rangle = \Theta_j^+(x_1) - \Theta_j^-(x_1), \tag{10}$$

where $j = 1, 3, 5$; $\Theta_j(z)$ are the functions analytic in the whole complex plane except the crack region $x_1 \in (c, b)$, $x_3 = 0$; $\langle \cdot \rangle$ means the jump of the function through the material interface; $m_{j5} = S_{j5}$, $m_{j1} = -iS_{j1}$, $n_{j1} = Y_{j1}$, $n_{j3} = -iY_{j3}$, $n_{j5} = -iY_{j5}$, $\mathbf{Y}_j = \mathbf{S}_j \boldsymbol{\rho}$; γ_j and $\mathbf{S}_j^T = [S_{j1}, S_{j3}, S_{j5}]$ are, respectively, the eigenvalues and eigenvectors of the matrix $(\gamma \ \boldsymbol{\rho}^T + \overline{\boldsymbol{\rho}}^T)$, where the matrix $\boldsymbol{\rho}$ is constructed from the matrix $\mathbf{G}$ of dimension 5×5 by crossing out the second and fourth rows and columns from this matrix; $\mathbf{G} = \mathbf{B}^{(1)} \mathbf{D}^{-1}$, $\mathbf{D} = \mathbf{A}^{(1)} - \overline{\mathbf{A}}^{(2)} (\overline{\mathbf{B}}^{(2)})^{-1} \mathbf{B}^{(1)}$, $\mathbf{A}^{(m)}$, $\mathbf{B}^{(m)}$ are matrixes similar to eponymous matrixes defined in [39] ($m = 1$ corresponds to the upper material and $m = 2$ – to the lower one).

When obtaining relations (9) and (10), the continuity of stresses, electric displacements and electric potential along the whole material interface were taken into account. Due to this fact the fourth row and column were excluded from the matrix $\mathbf{G}$ and also the case $j = 4$ was eliminated from Eqs. (9), (10).

Due to (9) the conditions at infinity for the function $\Theta_j(z)$ can be written in the form

$$\Theta_j(z)|_{z \to \infty} = (1 + \gamma_j)^{-1} (i \cdot m_{j1} \tau^{\infty} + \sigma^{\infty} + m_{j5} H^{\infty}). \tag{11}$$

3 Analytic Solution of the Problem

Due to relations (9) and (10) the interface conditions (6), (7) can be satisfied by the following relations:

$$\Theta_1^+(x_1) + \gamma_1\,\Theta_1^-(x_1) = 0 \text{ for } x_1 \in (c, a), \tag{12}$$

$$\Theta_5^+(x_1) + \Theta_5^-(x_1) = 0 \text{ for } x_1 \in (c, a), \tag{13}$$

and

$$\mathrm{Im}\big[\Theta_1^+(x_1) + \gamma_1\,\Theta_1^-(x_1)\big] = 0 \text{ for } x_1 \in (a, b), \tag{14}$$

$$\mathrm{Im}\big[\Theta_1^+(x_1) - \Theta_1^-(x_1)\big] = 0 \text{ for } x_1 \in (a, b), \tag{15}$$

In addition, for implementation of the relations

$$\langle u_3\rangle = 0,\ \langle W_3\rangle = 0 \text{ for } x_1 \in (a, b),$$

with the use of (10), we are able to require

$$\Theta_5^+(x_1) - \Theta_5^-(x_1) = 0 \text{ for } x_1 \in (a, b). \tag{16}$$

The last equation provides the analyticity of $\Theta_5(z)$ in (a, b).
Equations (14) and (15) lead to the following single relation

$$\mathrm{Im}\big[\Theta_1^\pm(x_1)\big] = 0 \text{ for } x_1 \in (a, b). \tag{17}$$

Thus, we arrive at the following combined Dirichlet-Riemann boundary value problem for the function $\Theta_1(z)$ analytic outside (c, b)

$$\Theta_1^+(x_1) + \gamma_1\,\Theta_1^-(x_1) = 0 \text{ for } x_1 \in (c, a), \tag{18}$$

$$\mathrm{Im}\big[\Theta_1^\pm(x_1)\big] = 0 \text{ for } x_1 \in (a, b) \tag{19}$$

and to the Hilbert problem for the function $\Theta_5(z)$ analytic outside (c, a)

$$\Theta_5^+(x_1) + \Theta_5^-(x_1) = 0 \text{ for } x_1 \in (c, a). \tag{20}$$

The conditions at infinity are

$$\Theta_1(z)|_{z\to\infty} = (1+\gamma_1)^{-1}(im_{11}\tau^\infty + \sigma^\infty + m_{15}H^\infty), \tag{21}$$

$$\Theta_5(z)|_{z\to\infty} = (1+\gamma_5)^{-1}(im_{51}\tau^{\infty} + \sigma^{\infty} + m_{55}H^{\infty}) = 0.5(\sigma^{\infty} + m_{55}H^{\infty}). \tag{22}$$

In the last equation we take into account that according to the numerical analysis $\gamma_5 = 1$ and $m_{51} = 0$.

The conditions at infinity can be expressed in the form

$$\Theta_j(z)|_{z\to\infty} = \tilde{\sigma}_j - i\tilde{\tau}_j, \tag{23}$$

where $\tilde{\sigma}_j = \frac{1}{r_j}(\sigma^{\infty} + m_{j5}H^{\infty})$, $\tilde{\tau}_j = -m_{j1}\tau^{\infty}/r_j$, $r_j = (1+\gamma_j)$, $j = 1, 5$.

An exact solution of the combined Dirichlet-Riemann boundary value problem (18), (19) obtained by using the paper [17] can be written as

$$\Theta_1(z) = P(z)X_1(z) + Q(z)X_2(z), \tag{24}$$

where

$$P(z) = C_1 z + C_2,\ Q(z) = U_1 z + U_2,\ X_1(z) = ie^{i\varphi(z)}/\sqrt{(z-c)(z-b)},$$
$$X_2(z) = e^{i\varphi(z)}/\sqrt{(z-c)(z-a)},\ l = b - c,$$
$$\varphi(z) = 2\varepsilon \ln\left[\frac{\sqrt{(b-a)(z-c)}}{\sqrt{(b-c)(z-a)} + \sqrt{(a-c)(z-b)}}\right],\ \varepsilon = \frac{1}{2\pi}\ln\gamma_1$$

and C_1, C_2, U_1, U_2 are real coefficients which can be found from the conditions at infinity (23) in the form

$$C_1 = -\tilde{\tau}_1\cos\beta - \tilde{\sigma}_1\sin\beta,\ U_1 = \tilde{\sigma}_1\cos\beta - \tilde{\tau}_1\sin\beta,$$
$$C_2 = -\frac{c+b}{2}C_1 - \beta_1 U_1,\ U_2 = \beta_1 C_1 - \frac{a+c}{2}D_1,$$

with

$$\beta = \varepsilon \ln\frac{1-\sqrt{1-\lambda}}{1+\sqrt{1-\lambda}},\ \beta_1 = \varepsilon\sqrt{(a-c)(b-c)} \text{ and } \lambda = \frac{b-a}{l}.$$

4 Analytical Expressions for the Components at the Interface

By using the solution (24) together with the formulas (9), (10) one can get the interface stresses for $x_1 > b$:

$$\sigma_{33}^{(1)}(x_1,0) + m_{14}H_{33}^{(1)}(x_1,0) + i\cdot m_{11}\sigma_{13}^{(1)}(x_1,0) = \\ = \left[\frac{Q(x_1)}{\sqrt{x_1-a}} + \frac{i\ P(x_1)}{\sqrt{x_1-b}}\right]\frac{r_1\exp[i\varphi(x_1)]}{\sqrt{x_1-c}}, \tag{25a}$$

the interface stresses and strain jumps for $x_1 \in L_2$:

$$\sigma_{33}^{(1)}(x_1,0)+m_{15}H_{33}^{(1)}(x_1,0)=\frac{r_1 P(x_1)}{\sqrt{(x_1-c)(b-x_1)}}\left[\frac{1-\gamma_1}{1+\gamma_1}\cosh\varphi_0(x_1)+\sinh\varphi_0(x_1)\right]+ \\ +\frac{r_1 Q(x_1)}{\sqrt{(x_1-c)(x_1-a)}}\left[\cosh\varphi_0(x_1)+\frac{1-\gamma_1}{1+\gamma_1}\sinh\varphi_0(x_1)\right] \tag{25b}$$

$$\left\langle u_1'(x_1,0)\right\rangle=\frac{1}{n_{11}\sqrt{x_1-c}}\left[\frac{P(x_1)}{\sqrt{b-x_1}}\cosh\varphi_0(x_1)+\frac{Q(x_1)}{\sqrt{x_1-a}}\sinh\varphi_0(x_1)\right], \tag{25c}$$

and the phonon and phason strain jumps for $x_1 \in L_1$:

$$n_{11}\left\langle u_1'(x_1,0)\right\rangle+i\left\{n_{13}\left\langle u_3'(x_1,0)\right\rangle+n_{15}\left\langle W_3'(x_1,0)\right\rangle\right\}= \\ =2\sqrt{\alpha}\left[\frac{P(x_1)}{\sqrt{b-x_1}}-i\,\frac{Q(x_1)}{\sqrt{a-x_1}}\right]\frac{\exp[i\varphi^*(x_1)]}{\sqrt{x_1-c}}, \tag{25d}$$

where

$$\varphi^*(x_1)=2\varepsilon\ln\left[\frac{\sqrt{(b-a)(x_1-c)}}{\sqrt{(b-c)(a-x_1)}+\sqrt{(a-c)(b-x_1)}}\right],$$
$$\varphi_0(x_1)=2\varepsilon\tan^{-1}\frac{\sqrt{(a-c)(b-x_1)}}{\sqrt{(b-c)(x_1-a)}},\ \alpha=\frac{(\gamma_1+1)^2}{4\gamma_1}.$$

By introducing phonon and phason stress intensity factors (SIFs)

$$k_1=\lim_{x_1\to a+0}\sqrt{2\pi(x_1-a)}\sigma_{33}^{(1)}(x_1,0),\ k_2=\lim_{x_1\to b+0}\sqrt{2\pi(x_1-b)}\sigma_{13}^{(1)}(x_1,0), \\ k_5=\lim_{x_1\to a+0}\sqrt{2\pi(x_1-a)}H_{33}^{(1)}(x_1,0), \tag{26}$$

one gets from the Eqs. (25a, 25b)

$$k_1+m_{15}k_5=\sqrt{\frac{\pi\ l}{2\alpha}}\,\omega_3, \tag{27a}$$

$$k_2=-\frac{1}{m_{11}}\sqrt{\frac{\pi\ l}{2\alpha}}\left[\omega_2+2\varepsilon\sqrt{1-\lambda}\omega_1\right], \tag{27b}$$

where $\omega_1=\sigma_d\cos\beta+m_{11}\tau\sin\beta$, $\omega_2=\sigma_d\sin\beta-m_{11}\tau\cos\beta$, $\omega_3=\omega_1\sqrt{1-\lambda}-2\varepsilon\omega_2$, $\sigma_d=\sigma^\infty+m_{15}H^\infty$.

The solution of the Hilbert problem (20) can be obtained by using the results of [40] as

$$\theta_5(z)=\frac{C_{04}+C_{14}z}{\sqrt{(z-c)(z-a)}} \tag{28}$$

and after defining the arbitrary coefficients C_{04}, C_{14} from the conditions (23), we get

$$\Theta_5(z) = \frac{\sigma_d'}{2}\left(z - \frac{c+a}{2}\right)\frac{1}{\sqrt{(z-c)(z-a)}}, \tag{29}$$

where $\sigma_d' = \sigma^{\infty} + m_{55}H^{\infty}$.

Using the relations (9) for $j = 5$ and taking into account that $m_{51} = 0$, it follows for $z = x_1 + i \cdot 0$ and for $x_1 > a$ the interface stress formula

$$\sigma_{33}^{(1)}(x_1, 0) + m_{55}H_{33}^{(1)}(x_1, 0) = \sigma_d'(x_1 - \frac{c+a}{2})\frac{1}{\sqrt{(x_1-c)(x_1-a)}}. \tag{30}$$

Further, using the definition (26) leads to

$$k_1 + m_{55}k_5 = \sigma_d'\sqrt{\pi(a-c)/2}. \tag{31}$$

In a similar way, from the Eqs. (10) with $j = 5$ one obtains for $z = x_1 + i \cdot 0$ and for $x_1 \in L_1$ the following jumps of the displacement derivatives:

$$\begin{aligned} n_{53}\langle u_3'(x_1, 0)\rangle + n_{55}\langle W_3'(x_1, 0)\rangle = \operatorname{Im}\{F_4^+(x_1) - F_4^-(x_1)\} = \\ = -\sigma_d'\left(x_1 - \tfrac{c+a}{2}\right)\tfrac{1}{\sqrt{(x_1-c)(a-x_1)}}. \end{aligned} \tag{32}$$

The phonon stress $\sigma_{33}^{(1)}(x_1, 0)$ and the phason stress $H_{33}^{(1)}(x_1, 0)$ for $z = x_1 + i \cdot 0$ can be easily determined from the Eqs. (25a) and (30) for $x_1 > b$ and from the Eqs. (25b) and (30) for $x_1 \in L_2$. The SIFs for $x_1 \to a + 0$ can be found from the Eq. (27a), which together with the Eq. (31) and by utilizing the relationship $(a - c) = l(1 - \lambda)$, leads to

$$k_1 = (m_{55} - m_{15})^{-1}\sqrt{\frac{\pi l}{2\alpha}}\left[[m_{55}\omega_3 - m_{15}\sigma_d'\sqrt{\alpha(1-\lambda)}\right], \tag{33a}$$

$$k_5 = -(m_{55} - m_{15})^{-1}\sqrt{\frac{\pi l}{2\alpha}}\left[\omega_3 - \sigma_d'\sqrt{\alpha(1-\lambda)}\right]. \tag{33b}$$

From the Eqs. (25d) and (32) one can easily find the expressions for $\langle u_3'(x_1, 0)\rangle$ and $\langle W_3'(x_1, 0)\rangle$ for $x_1 \in L_1$. Particularly for $x_1 \to a - 0$ these values have the following expressions

$$\langle u_3'(x_1, 0)\rangle = \frac{1}{2\sqrt{\gamma_1}\Delta_n}\sqrt{\frac{l}{a-x_1}}\left\{n_{44}\omega_3 - n_{14}\sigma_d'\sqrt{\gamma_1(1-\lambda)}\right\}, \tag{34a}$$

$$\langle W_3'(x_1, 0)\rangle = \frac{1}{2\sqrt{\gamma_1}\Delta_n}\sqrt{\frac{l}{a-x_1}}\left\{n_{53}\omega_3 - n_{13}\sigma_d'\sqrt{\gamma_1(1-\lambda)}\right\}, \tag{34b}$$

where $\Delta_n = n_{13}n_{55} - n_{53}n_{15}$.

Using the Eqs. (27a) and (31) allows to obtain the following expressions for $\left\langle u_3'(x_1, 0)\right\rangle$ and $\left\langle W_3'(x_1, 0)\right\rangle$ at the limit $x_1 \to a - 0$ via the IFs

$$\left\langle u_3'(x_1, 0)\right\rangle = -\frac{1}{\sqrt{2\pi(a - x_1)}}(\Theta_{11}k_1 + \Theta_{15}k_5), \tag{35a}$$

$$\left\langle W_3'(x_1, 0)\right\rangle = -\frac{1}{\sqrt{2\pi(a - x_1)}}(\Theta_{51}k_1 + \Theta_{55}k_5), \tag{35b}$$

where

$$\begin{array}{l}\Theta_{11} = (n_{44}\sqrt{\alpha/\gamma_1} - n_{14})/\Delta_n,\ \Theta_{15} = (m_{15}n_{55}\sqrt{\alpha/\gamma_1} - m_{55}n_{15})/\Delta_n,\\ \Theta_{51} = (n_{13} - n_{53}\sqrt{\alpha/\gamma_1})/\Delta_n,\ \Theta_{55} = (m_{55}n_{13} - m_{15}n_{43}\sqrt{\alpha/\gamma_1})/\Delta_n.\end{array} \tag{35c}$$

Moreover, for $x_1 \to b - 0$ Eq. (25c) leads to

$$\left\langle u_1'(x_1, 0)\right\rangle = -\frac{1}{\sqrt{2\pi(b - x_1)}}\Theta_{22}k_2, \tag{36}$$

with $\Theta_{22} = -\frac{2m_{11}}{n_{11}r_1}$.

Further, we introduce the energy release rates (ERRs) related to the points a and b:

$$G_1^c = \lim_{\Delta l \to 0}\frac{1}{2\Delta l}\int_a^{a+\Delta l}\left[\begin{array}{l}\sigma_{33}^{(1)}(x_1, 0)\langle u_3(x_1 - \Delta l, 0)\rangle\\ +H_{33}^{(1)}(x_1, 0)\langle W_3(x_1 - \Delta l, 0)\rangle\end{array}\right]dx_1, \tag{37a}$$

$$G_2^c = \lim_{\Delta l \to 0}\frac{1}{2\Delta l}\int_b^{b+\Delta l}\sigma_{31}^{(1)}(x_1, 0)\langle u_3(x_1 - \Delta l, 0)\rangle dx_1. \tag{37b}$$

Substituting the expressions $\sigma_{33}^{(1)}(x_1, 0)$, $H_{33}^{(1)}(x_1, 0)$, $\sigma_{31}^{(1)}(x_1, 0)$ from the defining Eq. (26) and by adopting the Eqs. (35a, 35b, 35c), (36) after the evaluation of the integrals (37a), (37b) one gets the following expressions:

$$G_1^c = [\Theta_{11}k_1^2 + \Theta_{55}k_5^2 + (\Theta_{15} + \Theta_{51})k_1k_5]/4, \tag{38a}$$

$$G_2^c = \Theta_{22}k_2^2/4. \tag{38b}$$

The total ERR can be found as

$$G = G_1^c + G_2^c = [\Theta_{11}k_1^2 + \Theta_{22}k_2^2 + \Theta_{55}k_5^2 + (\Theta_{15} + \Theta_{51})k_1k_5]/4.$$

5 Contact Zone Model and Numerical Illustration

The solution of an interface crack problem, as obtained in the previous chapter, is mathematically valid for any position of the point a. But for an arbitrary value of a it is not physically correct because for its physical validity the following inequalities

$$\sigma_{33}^{(1)}(x_1,0) \le 0 \text{ for } x_1 \in L_2,\ \langle u_3(x_1,0)\rangle \ge 0 \text{ for } x_1 \in L_1. \tag{39}$$

shall be satisfied. In this case, the contact zone model in Comninou's [16] sense takes place.

A corresponding analysis shows that these inequalities hold true if λ is taken from the segment $[\lambda_1, \lambda_2]$ where λ_1 is the maximum root from the interval (0,1) of the equation $\sqrt{a-x_1}\left\langle u_3'(x_1,0)\right\rangle = 0$ and λ_2 is the similar root of the equation $k_1 = 0$. By using the formulas (33a) and (34a) the equations for the determination of λ_1 and λ_2 can be written in the following shape, respectively

$$\omega_1 - \sqrt{\gamma_1}\frac{n_{15}}{n_{55}}\sigma_d' = \frac{2\varepsilon}{\sqrt{1-\lambda}}\omega_2 \tag{40a}$$

$$\omega_1 - \sqrt{\alpha}\frac{m_{15}}{m_{55}}\sigma_d' = \frac{2\varepsilon}{\sqrt{1-\lambda}}\omega_2. \tag{40b}$$

The confirmation of the fulfillment of inequalities (39) is presented in the Figs. 2 and 3, where the variation of $\langle u_3(x_1,0)\rangle$ in the interval $(b-b/5, a)$ and $\sigma_{33}^{(1)}(x_1,0)$ in (a,b), respectively, are presented for $c=-5$ mm, $b=5$ mm, $\sigma^\infty=0.1$ MPa, $\tau^\infty/\sigma^\infty=-30$, $H^\infty=30000$ Pa. For such a loading $\lambda_1=0.008755$ and $\lambda_2=0.05785$, graphs I in the Figs. 2 and 3 correspond to $\lambda=\lambda_1$, lines *II* – to $\lambda=(\lambda_1+\lambda_2)/2$ and line *III* – to $\lambda=\lambda_2$. It can be seen from these figures that for all considered values of λ the displacement jump $\langle u_3(x_1,0)\rangle$ remains positive and the stress $\sigma_{33}^{(1)}(x_1,0)$ in the contact zone holds negative, i.e. the inequalities (39) are satisfied and yield pressure along the contact line.

It is clear that for a certain loading the contact zone of unique length should take place. Definitely, this zone will correspond to the smooth crack closure, which occurs for $\lambda=\lambda_1$. The results relating to this case are depicted in the Figs. 4, 5 and 6. Particularly in Figs. 4 and 5 the variations of $\langle u_3(x_1,0)\rangle$ and $\langle W_3(x_1,0)\rangle$, respectively, in the interval (c,a) for the same $c,\ b,\ \sigma^\infty,\ \tau^\infty$ as in Figs. 2, 3 but for different H^∞ are shown. Curves *I* correspond to $H^\infty=38991.2$ Pa ($\lambda_1=\lambda_2=0.05823$), graphs II is drawn for $H^\infty=37041.6$ Pa ($\lambda_1=0.03923,\ \lambda_2=0.05815$) and line *III* correspond to $H^\infty=31192.9$ Pa ($\lambda_1=0.01135,\ \lambda_2=0.05790$).

It follows from the Figs. 4 and 5 that the phonon displacement jumps satisfy the second inequality (39) and always remains positive whilst $\langle W_3(x_1,0)\rangle$ change sign at the crack tip for some values of H^∞. However, such variation does not mean crack faces interpenetration because phason displacement $W_3(x_1,0)$ correspond to out of plane direction and is physically admissible. It is worth noting also that the lines *I*

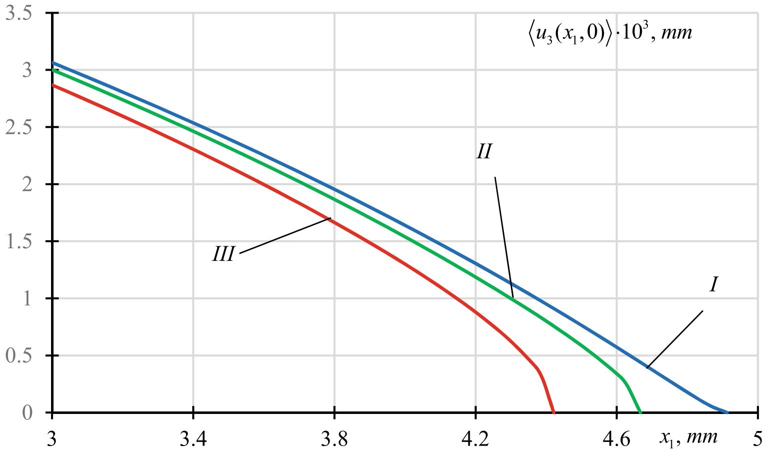

Fig. 2 The variation of $\langle u_3(x_1, 0)\rangle$ in the interval $(b-b/5, a)$ for $\sigma^\infty = 0.1$ *MPa*, $\tau^\infty/\sigma^\infty = -30$, $H^\infty = 30000$ *Pa*

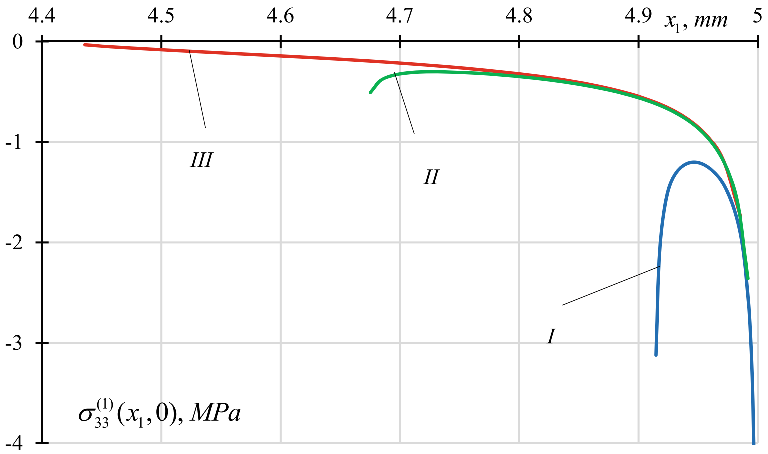

Fig. 3 The variation of $\sigma_{33}^{(1)}(x_1, 0)$ in the interval (a, b) for the same values of σ^∞, τ^∞ and H^∞ as in Fig. 2

correspond to the case of $\sigma'_d = 0$, which gives $\lambda_1 = \lambda_2$. In this case, according to (32), $\langle W_3(x_1, 0)\rangle$ is proportional to $\langle u_3(x_1, 0)\rangle$.

In Fig. 6 the variation of $H_{33}^{(1)}(x_1, 0)$ in the contact area (a, b) for the same c, b, σ^∞, τ^∞ as in Figs. 4 and 5 and different H^∞ are shown. The lines I, II and III in this Figure are also drawn for the same H^∞ as in Figs. 4 and 5.

It follows from the Fig. 6 that the obtained phason stress remains negative in the whole contact zone and only in the left end of this zone (point a in Fig. 1) it is equal

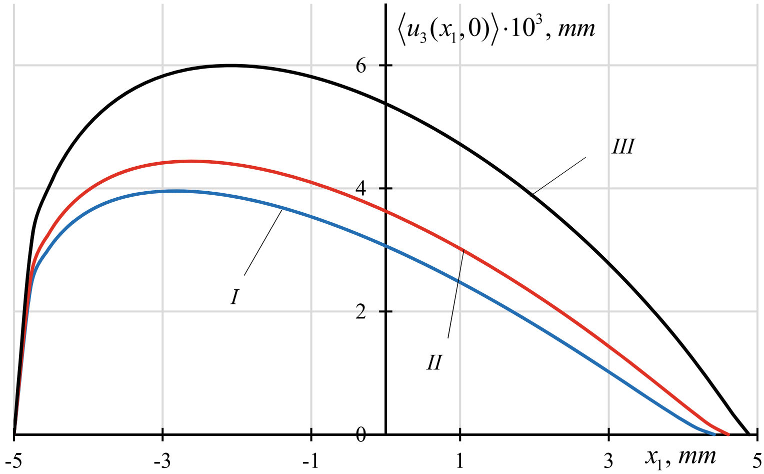

Fig. 4 The variation of the phonon crack opening $\langle u_3(x_1, 0)\rangle$ in the interval (c, a) for the same crack length and loading as in Fig. 2 and different values of H^{∞}

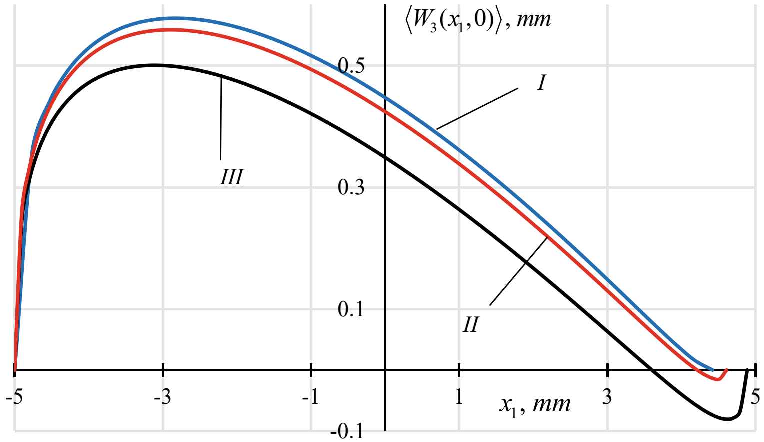

Fig. 5 The variation of the phason crack faces jump $\langle W_3(x_1, 0)\rangle$ in the interval (c, a) for the same parameters as in Fig. 4

to zero for $\sigma_d' = 0$ (line I). It is worth also to be mentioned that for $\sigma_d' = 0$, according to (30), one gets $\lambda_1 = \lambda_2$ and $H_{33}^{(1)}(x_1, 0)$ in this case is proportional to $\sigma_{33}^{(1)}(x_1, 0)$.

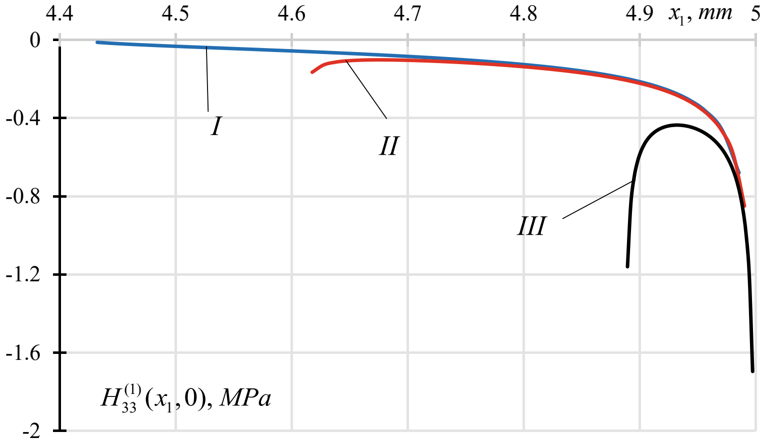

Fig. 6 The variation of the phason stress $H_{33}^{(1)}(x_1, 0)$ in the contact area (a, b) for the same parameters as in Fig. 4

6 Conclusions

A plane problem for an interface crack between two piezoelectric quasicrystalline half spaces under remote loading is considered. The stresses and electrical displacements as well as the derivatives of the displacement and electrical potential jumps are presented via a sectionally holomorphic vector function. This vector-function is analytically continued across the mechanically and electrically bonded parts of the material interface.

Further on, introducing an artificial frictionless contact zone at the right crack tip and by assuming the electrically permeable crack faces assumption the problem is reduced to a combined Dirichlet-Riemann boundary value problem. An exact analytical solution of this problem is derived. On the base of this solution the phonon and phason stresses as well as derivatives of the phonon and phason displacement jumps along the correspondent parts of the material interface are expressed in a clear analytical form. The stress intensity factors and the energy release rates at the singular points are found.

The contact zone model (in Comninou's sense) is derived as a particular case of the obtained solution. Transcendental equations are found for the determination of the real contact zone length. It is shown that for a remote tensile stress the real contact zone length is extremely small, but for an essential shear field it becomes longer and even comparable with the crack length.

Acknowledgements The Author V. Loboda is very grateful for the financial support from DAAD, thanks to which he had the pleasure of working under Professor's Herrmann guidance in 1996, 2000, 2004 and 2008. The Author V. Govorukha would like to express his gratitude for the support of the Alexander von Humboldt Foundation.

References

1. Shechtman, D., Blech, I., Gratias, D., Cahn, J.W.: Metallic phase with long-range orientational order and no translational symmetry. Phys. Rev. Lett. **53**, 1951–1953 (1984)
2. Fan, T.Y.: Mathematical Theory of Elasticity of Quasicrystals and Its Applications. Springer, Beijing (2011)
3. Steurer, W., Deloudi, S.: Crystallography of Quasicrystals: Concepts, Methods and Structures. Springer Series in Materials Science, vol. 126 (2009)
4. Fan, T.Y., Mai, Y.W.: Elasticity theory, fracture mechanics and some relevant thermal properties of quasicrystal materials. Appl. Mech. Rev. **57**, 325–344 (2004)
5. Li, X.F., Sun, Y.F., Fan, T.Y.: Elastic field of a straight dislocation in one dimensional hexagonal quasicrystals. J. Beijing Inst. Technol. **8**, 65–70 (1999)
6. Gao, Y., Ricoeur, A., Zhang, L.L.: Plane problems of cubic quasicrystal media with an elliptic hole or a crack. Phys. Lett. A **375**, 2775–2781 (2011)
7. Liu, G.T., Guo, R.P., Fan, T.Y.: On the interaction between dislocations and cracks in one dimensional hexagonal quasi-crystals. Chin. Phys. B **12**, 1149–1155 (2003)
8. Li, X.Y.: Elastic field in an infinite medium of one-dimensional hexagonal quasicrystal with a planar crack. Int. J. Solids Struct. **51**, 1442–1455 (2014)
9. Wang, Z., Ricoeur, A.: Numerical crack path prediction under mixed-mode loading in 1D quasicrystals. Theoret. Appl. Fract. Mech. **90**, 122–132 (2017)
10. Zhang, L., Wu, D., Xu, W., Yang, L., Ricoeur, A., Wang, Z., Gao, Y.: Green's functions of one-dimensional quasicrystal bi-material with piezoelectric effect. Phys. Lett. A **380**, 3222–3228 (2016)
11. Li, X.Y., Li, P.D., Wu, T.H., Shi, M.X., Zhu, Z.W.: Three-dimensional fundamental solutions for one-dimensional hexagonal quasicrystal with piezoelectric effect. Phys. Lett. A **378**, 826–834 (2014)
12. Fan, C.Y., Li, Y., Xu, G.T., Zhao, M.H.: Fundamental solutions and analysis of three-dimensional cracks in one-dimensional hexagonal piezoelectric quasicrystals. Mech. Res. Commun. **74**, 39–44 (2016)
13. Zhou, Y.B., Li, X.F.: Fracture analysis of an infinite 1D hexagonal piezoelectric quasicrystal plate with a penny-shaped dielectric crack. Eur. J. Mech./A Solids **76**, 224–234 (2019)
14. Yang, J., Zhou, Y.T., Ma, H.L., Ding, S.H., Li, X.: The fracture behavior of two asymmetrical limited permeable cracks emanating from an elliptical hole in one-dimensional hexagonal quasicrystals with piezoelectric effect. Int. J. Solids Struct. **108**, 175–185 (2017)
15. Williams, M.L.: The stresses around a fault or cracks in dissimilar media. Bull. Seismol. Soc. Am. **49**, 199–204 (1959)
16. Comninou, M.: The interface crack. J. Appl. Mech. **44**, 631–636 (1977)
17. Herrmann, K.P., Loboda, V.V.: On interface crack models with contact zones situated in an anisotropic bimaterial. Arch. Appl. Mech. **69**, 317–335 (1999)
18. Herrmann, K.P., Loboda, V.V.: Fracture mechanical assessment of electrically permeable interface cracks in piezoelectric bimaterials by consideration of different contact zone models. Arch. Appl. Mech. **70**, 127–143 (2000)
19. Herrmann, K.P., Govorukha, V.B., Loboda, V.V.: On contact zone model for an interface crack with electrically insulated crack surfaces in a piezoelectric bimaterial. Int. J. Fracture **11**, 203–227 (2001)
20. Herrmann, K.P., Loboda, V.V., Khodanen, T.V.: An interface crack with contact zones in a piezoelectric/piezomagnetic bimaterial. Arch. Appl. Mech. **80**(6), 651–670 (2010)
21. Herrmann, K.P., Loboda, V.V.: Contact zone models for an interface cracks in a thermomechanically loaded anisotropic bimaterial. J. Therm. Stress. **24**(5), 479–506 (2001)
22. Herrmann, K.P., Loboda, V.V.: Fracture mechanical assessment of interface cracks with contact zones in piezoelectric bimaterials under thermoelectromechanical loadings I. Electrically permeable interface cracks. Int. J. Solids Struct. **40**, 4191–4217 (2003)

23. Herrmann, K.P., Loboda, V.V.: Fracture mechanical assessment of interface cracks with contact zones in piezoelectric bimaterials under thermoelectromechanical loadings II. Electrically impermeable interface cracks. Int. J. Solids Struct. **40**, 4219–4237 (2003)
24. Herrmann, K.P., Loboda, V.V., Komarov, A.V.: Contact zone assessment for a fast growing interface crack in an anisotropic bimaterial. Arch. Appl. Mech. **74**, 118–129 (2004)
25. Herrmann, K.P., Loboda, V.V., Komarov, O.V.: On a moving interface crack with a contact zone in a piezoelectric bimaterial. Int. J. Solids Struct. **42**, 4555–4573 (2005)
26. Lapusta, Y., Komarov, A., Labesse-Jied, F., Moutou Pitti, R., Loboda, V.: Limited permeable crack moving along the interface of a piezoelectric bi-material. Europen J. Mech. A/Solids **30**, 639–649 (2011)
27. Govorukha, V.B., Loboda, V.V., Kamlah, M.: On the influence of the electric permeability on an interface crack in a piezoelectric bimaterial compound. Int. J. Solids Struct. **43**, 1979–1990 (2006)
28. Loboda, V., Lapusta, Y., Sheveleva, A.: Limited permeable crack in an interlayer between piezoelectric materials with different zones of electrical saturation and mechanical yielding. Int. J. Solids Struct. **47**, 1795–1806 (2010)
29. Sheveleva, A., Lapusta, Y., Loboda, V.: Zones of opening and closing for an interface crack in a piezoelectric bimaterial under tension-compression and shear loading. Mech. Res. Commun. **63**, 6–12 (2015)
30. Govorukha, V., Kamlah, M., Sheveleva, A.: Influence of concentrated loading on opening of an interface crack between piezoelectric materials in a compressive field. Acta Mech. **226**, 2379–2391 (2015)
31. Viun, O., Komarov, A., Lapusta, Y., Loboda, V.: A polling direction influence on fracture parameters of a limited permeable interface crack in a piezoelectric bi-material. Eng. Fract. Mech. **191**, 143–152 (2018)
32. Zhao, M.H., Dang, H.Y., Fan, C.Y., Chen, Z.T.: Analysis of a three-dimensional arbitrarily shaped interface crack in a one-dimensional hexagonal thermo-electro-elastic quasicrystal bi-material, Part 1: Theoretical solution. Eng. Fract. Mech. **179**, 59–78 (2017)
33. Zhao, M.H., Dang, H.Y., Fan, C.Y., Chen, Z.T.: Analysis of a three-dimensional arbitrarily shaped interface crack in a one-dimensional hexagonal thermo-electro-elastic quasicrystal bi-material, Part 2: numerical method. Eng. Fract. Mech. **180**, 268–281 (2017)
34. Loboda, V., Komarov, O., Bilyi, D., Lapusta, Y.: An analytical approach to the analysis of an electrically permeable interface crack in a 1D piezoelectric quasicrystal. Acta Mech. **231**, 3419–3433 (2020)
35. Loboda, V., Sheveleva, A., Komarov, O., Chapelle, F., Lapusta Y.: Arbitrary number of electrically permeable cracks on the interface between two one-dimensional piezoelectric quasicrystals with piezoelectric effect. Eng. Fracture Mech. **276**(A), 108878 (2022)
36. Hu, K.Q., Jin, H., Yang, Z., Chen, X.: Interface crack between dissimilar one-dimensional hexagonal quasicrystals with piezoelectric effect. Acta Mech. **230**, 2455–2474 (2019)
37. Loboda, V., Sheveleva, A., Komarov, O., Lapusta, Y.: An interface crack with mixed electrical conditions at it faces in 1D quasicrystal with piezoelectric effect. Mech. Adv. Mater. Struct. **29**(23), 3334–3344 (2022)
38. Hu, K.Q., Gao, C.-F., Zhong, Z., Chen, Z.T.: Interaction of collinear interface cracks between dissimilar one-dimensional hexagonal piezoelectric quasicrystals. Z. Angew. Math. Mech. **101**, e202000360 (2021)
39. Suo, Z., Kuo, C.M., Barnett, D.M., Willis, J.R.: Fracture mechanics for piezoelectric ceramics. J. Mech. Phys. Solids **40**, 739–765 (1992)
40. Muskhelishvili, N.I.: Some Basic Problems of the Mathematical Theory of Elasticity. Noordhoff, Groningen (1975)